

Research Article

Accurate Empirical Path Loss Models with Route Classification for mmWave Communications

Supachai Phaiboon ¹ and Pisit Phokharatku²

¹Department of Electrical Engineering, Faculty of Engineering, Mahidol University, Phuttamonthon 4 Road, Salaya, Phuttamonthon, Nakhon Pathom 73170, Thailand

²Department of Electrical Engineering and Energy Management, Faculty of Engineering, Kasem Bundit University, Pattanakarn Road, Suanluang, Bangkok 10250, Thailand

Correspondence should be addressed to Supachai Phaiboon; supachai.pai@mahidol.ac.th

Received 28 June 2022; Revised 31 August 2022; Accepted 19 September 2022; Published 20 October 2022

Academic Editor: Ravi Gangwar

Copyright © 2022 Supachai Phaiboon and Pisit Phokharatku. This is an open access article distributed under the Creative Commons Attribution License, which permits unrestricted use, distribution, and reproduction in any medium, provided the original work is properly cited.

This paper presents accurate empirical path loss models with route classification for the high band frequency of 5G wireless. Propagation path routes are mainly classified into line of sight (LOS) and non-line-of-sight (NLOS). The NLOS routes are classified into 2 separate routes, namely, Hard_NLOS and Soft_NLOS. Their path loss models include free-space loss (L_f) and multiscreen diffraction loss (L_{msd}) together with the reflection from the building blocks. However, these NLOS routes can be combined into a single formula. The path loss models were fitted with measured path loss data at frequencies of 28 GHz and 73 GHz. These models are compared with four 5G empirical models, namely 5GCM, 3GPP, METIS, and mmMAGIC. The results show that the separated route models provide good agreement, especially for the hard routes compared with those models and provide the minimum MAE of 4.45 dB, 4.34 dB, and 6.72 dB for the hard route, soft route, and an all-NLOS route, respectively, for the dual-band frequency.

1. Introduction

Wireless data transmission has been increasing with the rise of the Internet of Things (IoT) and high-speed movie downloads. The IoT has found its wide applications, including the application of smart cities, smart health care systems, intelligent transportation, climate monitoring, smart farming, and industrial robots. The above networks need very high-performance communications and stability. Therefore, the fifth generation (5G) of mobile communications challenges daily life to the new normal, including working from home. The propagation path loss models for millimeter waves in high band frequencies (above 24 GHz) are an important thing for connecting the communication of both 5G nonstand alone and 5G standalone networks.

1.1. Background and Related Works. There are three types of path loss models that are commonly used, namely empirical

model, semideterministic model, and deterministic model. The empirical models developed from an intensive measurements of 5G [1, 2] are often used since they need only frequency, path loss exponent (PLE), and distance to compute the path loss for macro and microcell planning. In [1–3], the PLEs are provided for the frequencies of 28 GHz, 38 GHz, 60 GHz, and 73 GHz. The probabilistic model was proposed based on the probability distribution for the line of sight (LOS) and non-line-of-sight (NLOS) at 1 m close-in free space reference distance (CI) model and the floating-intercept model (FI) [4]. The three large-scale path loss models [5] are investigated, namely, the Alpha-Beta-Gamma (ABG) model, the CI model, and the CI model with a frequency-weighted path loss exponent (CIF). The comparison of these models is discussed. In [6], path loss models are discussed for urban street canyons both floating intercept (FI) and fixed reference (FR) at frequencies of 0.8 to 60.4 GHz. Correction factors [7] are modified for CI path loss models at 60 GHz and 73 GHz for both LOS and NLOS

scenarios. In [8], the fitting the path loss model used weighted distances and censored path loss data in order to improve the accuracy of prediction at a frequency of 28 GHz. Also, in [9], ray-tracing simulations together with measurements are used to model 28 GHz empirical path loss. An overview of empirical path loss models is discussed in [2] for LOS and NLOS millimeter waves in both indoor and outdoor environments. Two slope path loss models with critical distances are analyzed and the high performance for application is shown [10]. The path loss models provide more accurate predictions compared with the single slope path loss models. Additionally, path loss models with two frequency bands are applied for improving localization of WSN [11].

The second type, the semideterministic models are also often used since they need not only the parameters of the empirical models but also some information about the propagation path, such as the propagation route, the height of the building, the distance between the mobile device and the last building, and the width of the road. These models provide accurate path loss and are used for planning or solving the communication network. For semideterministic models, there are previous studies. Xia et al. [12, 13] proposed path loss formulas for microcells in low-rise and high-rise building environments at frequencies of 0.9 to 2.0 GHz. This model classified the NLOS routes and provided the individual models together with an all-NLOS model. The COST 231 WI model [14–17] is also a popular prediction tool for microcell environments at frequencies of 0.8 GHz to 2.0 GHz. Guan et al. [18] proposed an advanced Hata model, including obstacles with Fresnel parameters that are used to determine the path loss of a high-speed railway. Bhuvaneshwari et al. [19] proposed a hybrid WI model by including multiple reflection loss from ray tracing. Wang et al. [20] proposed a semideterministic model at a semideterministic model at a frequency of 5.2 GHz by using a theory of diffraction at the roof top of the building. Karttunen et al. [21] proposed NLOS propagation behind the second diffraction and modelled the path loss at a frequency of 28 GHz. However, this model is complex and difficult to use. Additionally, a multihop data routing with reinforcement learning method has been proposed for IOT networks [22]. This research shows a high performance in terms of energy efficiency and quality of service (QoS). Intelligent surfaces are applied to reduce path loss in NLOS routes on the mmWave communications [23].

Finally, in the last type, the deterministic models need details of digitized maps and materials of buildings, which take a lot of time for computing. There are path loss models based on theory [24, 25]. These models are also often used to calibrate empirical models [8, 9] and semideterministic models [19, 21].

1.2. Contributions. Although the above empirical models [1, 2] are popular used, however, they provide large errors in the case of full obstruction between transmitter and receiver. The semideterministic models [12–21] are provide an accuracy prediction, however, they need details of the propagation

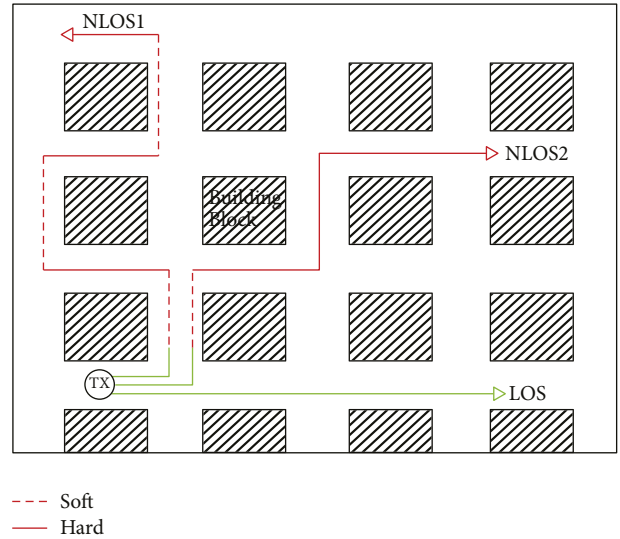


FIGURE 1: LOS and NLOS routes in street canyon (idealized scenario).

scenario for calculation such as building height, width of road, and distance between receiver and the last building, and so on. In order to solve the above problems, this paper proposes path loss models that are separated the NLOS routes to provide an accuracy path loss prediction. The convectional Xia model [12] was modified to classify the propagation routes, namely, the soft route and the hard route. The researcher proposed path loss modeling with route classification at frequency of 28 GHz and 73 GHz for 5G networks. Section 2 presents accurate path loss models. Section 3 presents path loss data. Section 4 results and discussions are presented. Finally, Section 5 presents conclusions.

2. Accurate Path Loss Models

An empirical path loss model for urban environment was applied to predict path loss by using 3D maps of buildings. Propagation path routes are mainly classified into line of sight (LOS) and non-line-of-sight (NLOS). The NLOS routes are classified into 2 routes, namely, hard and soft routes.

Soft routes as shown in Figure 1. In the case of the hard route, the transmitting waves diffract at several corners of the buildings, as shown by the solid red line in Figure 1. This makes the path loss very high, while in the case of the soft route, the transmitting waves diffract at only one corner, as shown by the dotted red lines in Figure 1. However, the soft route may become a hard route when there are trees in the route, while the hard route will become a soft route when the dominant wave propagates via open buildings. For low-rise building environments in which base station antennas are near to or above the roof tops of the buildings, the wave propagation takes place around the roof tops through diffractions and reflections at the building surfaces as shown in Figure 2(a). While the high-rise building environment or low antenna height in which base station antennas are below the tops of the surrounding buildings, the propagation takes place around the sides of the buildings through reflections at

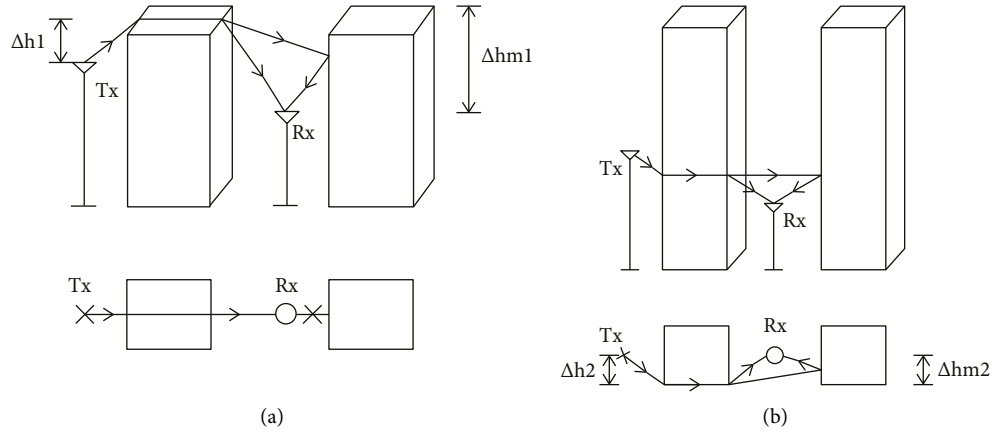


FIGURE 2: Mechanism of diffraction around the buildings. (a) Over rooftop. (b) Building corner.

the building surfaces and diffractions at the building corners, as shown in Figure 2(b). The total path losses can be approximated as a sum of the free-space loss (L_{fs}) and the multiscreen diffraction loss. There are two types of path loss modes, namely, CI model and ABG model.

The path loss generally consists of two theory fixed terms, called “Close-in free space reference distance (CI)” including one parameter (n) needs to be optimization.

$$PL(d) = C1_i + C2_i \log(f_G) + C3_i \log(d_{3D}), \quad (1)$$

where d_{3D} is the mobile 3D Euclidean distance from transmitter (m), f_G is frequency in GHz, $C1_i$ and $C2_i$ are fixed arbitrary constants and $C3_i/10$ is path loss exponent (PLE, n). Subscripts i are the numbers of 1 to 3 for hard, soft and all-NLOS routes respectively. However, LOS in the urban area has a wave guiding effect from a street canyon with surrounding buildings. The fixed terms do not match the theory and depend on the environment.

2.1. ABG Model. The path loss consists of sum of 3 terms arbitrary constants, namely, Alpha (α), Beta (β), and Gamma (γ),

$$PL(d) = 10\alpha_i \log(d_{3D}) + \beta_i + 10\gamma_i \log(f_G), \quad (2)$$

where d_{3D} is the mobile 3D distance from transmitter (m), f_G is the frequency (GHz). Subscripts i are the numbers of 1 to 3 for hard, soft, and all-NLOS routes, respectively.

3. Path Loss Data

The researchers used measured path loss data in the dense urban environment around New York University’s (NYU) campus area in Manhattan, NY, USA, based on a three-dimensional building as shown in Figures 3 and 4 for modeling [26]. The measurements were performed for a microcell by omnidirectional large-scale LOS and NLOS. The 28 GHz transmitters were located at three sites on the buildings at 7 and 17 m. above ground, as shown by yellow star marks in Figure 3, while the 73 GHz transmitters were located at five sites on the buildings at 7 and 17 m. above ground, as shown by the yellow star marks in Figure 4. A

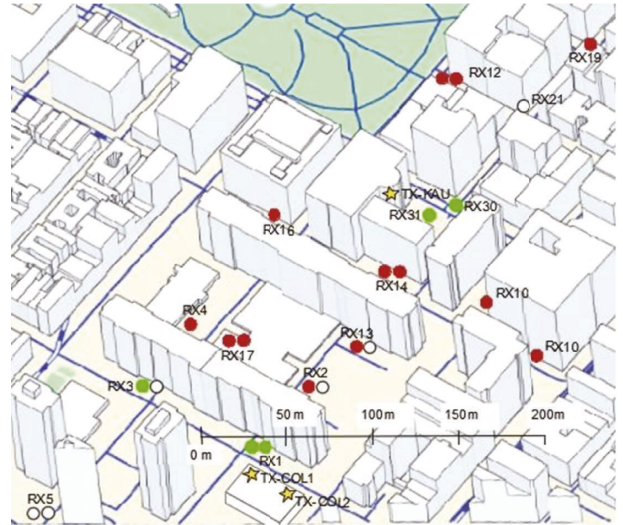


FIGURE 3: 3D building map of TX and RX locations around an urban area for 28 GHz measurements; stars indicate TX locations and dots indicate RX locations.



FIGURE 4: 3D building map of TX and RX locations around an urban area for 73 GHz measurements; stars indicate TX locations and dots indicate RX locations.

TABLE 1: Summary of the measurement parameters.

Frequency (GHz)	Tx (m)	Rx (m)	Route	Number of locations	PL (dB)		
					Min.	Max.	
28	7-17	1.5	LOS	5	88.4	100.8	
			NLOS				
			(i) Hard	14	118	149.2	
			(ii) Soft	6	115.6	124.8	
73	7-17	2-4	LOS	9	97.8	108.4	
			NLOS				
			(i) Hard	31	132	159.7	
			(ii) Soft	22	117.4	145.9	

total of 96 path loss data points were recorded for the frequencies of 28 GHz and 73 GHz. A total of totally 87 path loss data points were used for modeling. The receiver moved along the road at 1.5, 2, and 4.06 m above ground (circular dots) within a 590 m × 550 m area. The road width is about 20 m from the front of the building beside the road. Most buildings in the area are about 20–60 m high, with an average of about 53.1 m, and a building density of about 65% in the area. In this paper, the parameters for path loss modeling are the propagation routes and 3D distance between the transmitter and the receiver. The LOS routes, as shown by green dots in Figures 3 and 4, are in the street canyon and beside the buildings, with minimum and maximum ranges of 31 m. and 102 m., respectively. The researchers classify NLOS routes into 2 categories, namely hard and soft NLOSs. The hard NLOS consists of transverse and staircase routes which are NLOS streets behind two corners of one or two buildings, as shown by the red dots in Figures 3 and 4. While the soft NLOS, or the lateral routes, are NLOS streets from only one corner of a building, as shown by white dots in Figures 3 and 4. The PL values of hard NLOS with higher frequency are generally higher than soft NLOS as shown in Table 1. The maximum distance in this measurement is 186 m. with a PL of 149.2 dB and a frequency of 28 GHz. In the case of 73 GHz, the maximum distance is 182 m. with PL of 156.2 dB. This confirms that path loss modeling can be used for 5G microcells. All distances are 2D or horizontal distance, which can be transformed to 3D with relative antenna heights for path loss modeling.

4. Results and Discussions

The researchers proposed path loss models by fitting the classified PL data. The PL models will be the close-in free space reference distance (CI) path loss model (with a 1 m reference distance) for narrow bands and dual band frequency (28 GHz and 73 GHz) for high-rise buildings, which influence the dominant path of wave travel.

4.1. Single Frequency CI Models

4.1.1. Frequency of 28 GHz

$$PL_{\text{LOS}_{28}}(d) = 32.4 + 20 \log f_G + 20.5 \log d_{3D}. \quad (3)$$

$$PL_{\text{softNLOS}_{28}}(d) = 32.4 + 20 \log f_G + 27.3 \log d_{3D}. \quad (4)$$

TABLE 2: Summary of the CI arbitrary constants 28 GHz.

Path type	Route	Arbitrary constant			MAE
		C1	C2	C3	ϵ
LOS	All	32.4	20	20.5	3.17
	Hard	32.4	20	36.6	5.04
NLOS	Soft	32.4	20	27.3	3.52
	All	32.4	20	33.9	7.51

TABLE 3: Summary of the CI arbitrary constants of 73 GHz.

Path type	Route	Arbitrary constant			MAE
		C1	C2	C3	ϵ
LOS	All	32.4	20	20.9	4.38
	Hard	32.4	20	37.1	4.2
NLOS	Soft	32.4	20	31.0	3.76
	All	32.4	20	34.0	6.47

$$PL_{\text{hardNLOS}_{28}}(d) = 32.4 + 20 \log f_G + 36.6 \log d_{3D}. \quad (5)$$

$$PL_{\text{allNLOS}_{28}}(d) = 32.4 + 20 \log f_G + 33.9 \log d_{3D}. \quad (6)$$

4.1.2. Frequency of 73 GHz.

$$PL_{\text{LOS}_{73}}(d) = 32.4 + 20 \log f_G + 20.9 \log d_{3D}. \quad (7)$$

$$PL_{\text{softNLOS}_{73}}(d) = 32.4 + 20 \log f_G + 31 \log d_{3D}. \quad (8)$$

$$PL_{\text{hardNLOS}_{73}}(d) = 32.4 + 20 \log f_G + 37.1 \log d_{3D}. \quad (9)$$

$$PL_{\text{allNLOS}_{73}}(d) = 32.4 + 20 \log f_G + 34 \log d_{3D}. \quad (10)$$

Path losses for each frequency are shown in equations (3)–(10) and summarized in Tables 2 and 3. The LOS path loss generally provides a constant C2 of 2.0 at both frequencies. However, the path loss exponent n increases from 2.0 due to obstruction effects along the street canyons, especially at higher frequencies. The model provides a maximum prediction error of 3.23 dB at the frequency of 73 GHz because of the scattering from many objects at a small wavelength.

While at a frequency of 28 GHz, it provides a minimum error of 3.17 dB. This is because of the influence of wave scattering at the lower frequency. In the case of NLOS, the

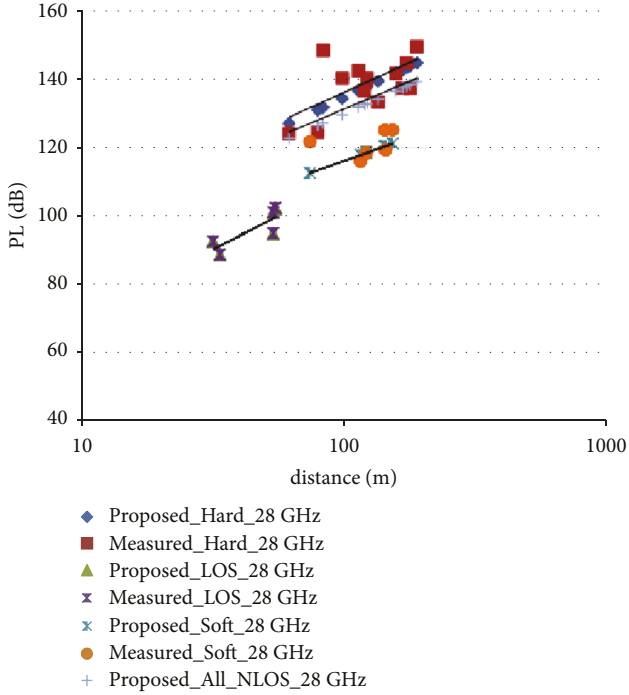


FIGURE 5: Proposed Model at frequency of 28 GHz.

PLE (n) of the hard routes generally provide the highest values because of multidiffraction at the building and/or vegetation. While all-NLOS provides PL in the range between hard and soft routes (Figures 5–7). However, all models provide the confidential interval within the accepted value of 8 dB.

4.2. Dual Frequency (28 GHz and 73 GHz)

4.2.1. CI

$$PL_{LOS}(d) = 32.4 + 20 \log f_G + 20.6 \log d_{3D}. \quad (11)$$

$$PL_{soft}(d) = 32.4 + 20 \log f_G + 29.0 \log d_{3D}. \quad (12)$$

$$PL_{hard}(d) = 32.4 + 20 \log f_G + 36.8 \log d_{3D}. \quad (13)$$

$$PL_{allNLOS}(d) = 32.4 + 20 \log f_G + 34.1 \log d_{3D}. \quad (14)$$

4.2.2. ABG

$$L_{softNLOS}(d) = 35.11 \log(d_{3D}) + 21.6 + 21.5(f_G), \quad (15)$$

$$PL_{hardNLOS}(d) = 36.4 \log(d_{3D}) + 31.4 + 20.9 \log(f), \quad (16)$$

$$L_{allNLOS}(d) = 37.5 \log(d_{3D}) + 22.4 + 21.4 \log(f). \quad (17)$$

The dual frequency path loss models are shown in equations (11)–(17) and summarized in Table 4. The path loss exponents of all equations have the same trend as the single frequency above. Additionally, the errors of these

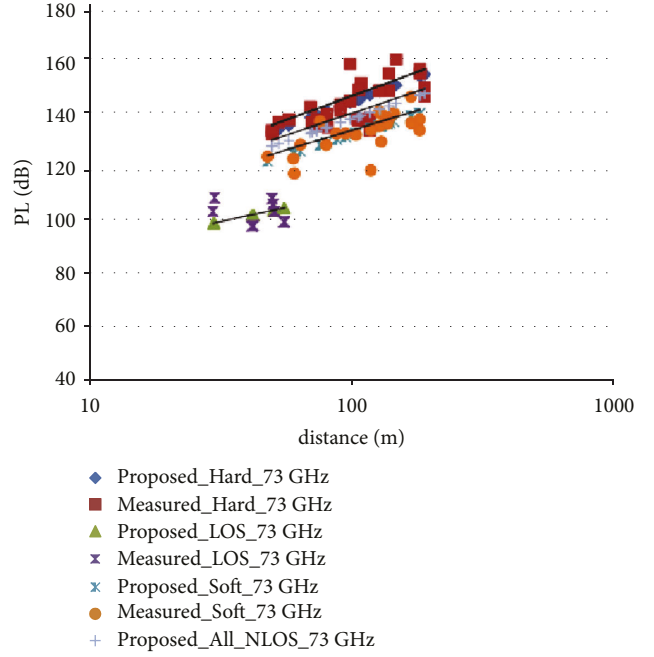


FIGURE 6: Proposed Model at frequency of 73 GHz.

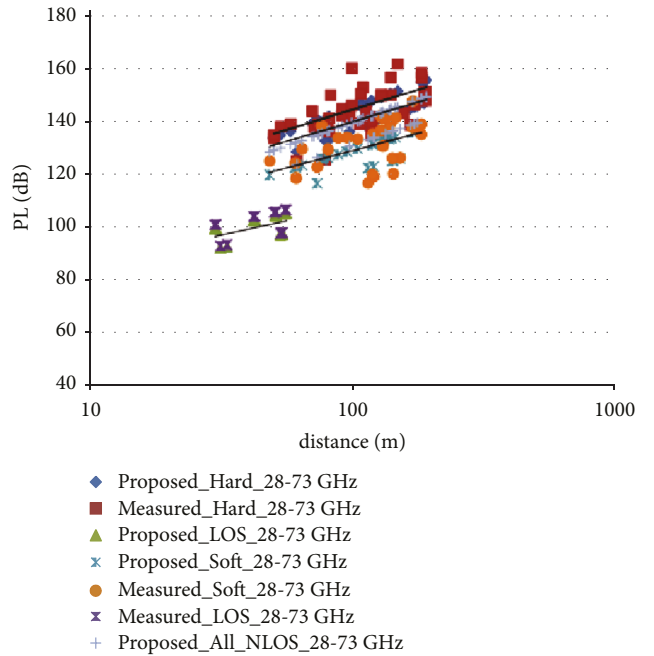


FIGURE 7: Proposed Model at frequency of 28 and 73 GHz.

TABLE 4: Summary of the CI and ABG arbitrary constants of dual frequency.

Path type	Route	Arbitrary constant			MAE
		C1(α)	C2(β)	C3(γ)	ϵ
LOS	All	32.4	20.0	20.6	3.89
	Hard	32.4 (3.64)	20 (31.4)	36.8 (2.09)	4.46 (4.45)
NLOS	Soft	32.4 (3.41)	20 (32.4)	29.0 (2.0)	4.34 (4.38)
	All	32.4 (3.75)	20 (22.4)	34.1 (2.14)	6.72 (6.78)

TABLE 5: Comparison of LOS path loss models.

Name	LOS models	MAE	σ
5GCM UMi street canyon	$PL = 32.4 + 20 \log(f) + 21 \log(d_{3D})$ $PL_1 = 32.4 + 20 \log(f) + 21 \log(d_{3D})$ $PL_2 = 32.4 + 40 \log(d_{3D})$	3.23	2.61
3GPP UMi street canyon	$+20 \log(f) - 9.5 \log(d_{bp}^2) - (h_b - h_m)^2$ <i>where</i> $d_{bp} = 4h_b h_m / \lambda$ $PL_1 = 31.34 + 20 \log(f) - 1.38 \log(f) + 22 \log(d_{3D})$ $10m \leq d_{3D} \leq d_{bp}$ where, d_{bp} $= 0.87 \exp(-\log(f))4(h_{BS} - 1m)(h_{UE} - 1m)/(0.65\lambda)$	3.23	2.61
METIS	$PL = 31.34 + 20 \log(f) - 1.38 \log(f) + 22 \log(d_{3D})$ $= 0.87 \exp(-\log(f))4(h_{BS} - 1m)(h_{UE} - 1m)/(0.65\lambda)$	3.27	2.66
mmMAGIC	$PL = 32.4 + 20.8 \log(f) + 19.2 \log(d_{3D})$	3.28	2.33
Proposed (28 GHz)	$PL = 32.4 + 20 \log(f) + 20.5 \log(d_{3D})$	3.17	1.97
Proposed (73 GHz)	$PL = 32.4 + 20 \log(f) + 20.9 \log(d_{3D})$	3.23	2.35
Proposed (28–73 GHz)	$PL = 32.4 + 20 \log(f) + 20.6 \log(d_{3D})$	3.2	2.7

models are within the range of the accepted interval (within 8 dB). However, the errors of LOS models (3.2 dB) decrease from the averaging of the single frequency. For NLOS, some measurement points of a soft route which are defined in Section 2, become a hard route. This is because there is vegetation or objects around the measurement point, as shown in Figure 4 by the white dots (RX26 and RX27). On the other hand, some measurement points of the hard route become soft routes (RX19) with the red dot in Figure 4 because of the open building on the first floor. This makes the waves propagate via the building blocks.

4.3. Comparison of Models. In order to compare the accurate models with other models, four models are used, namely, 5GCM, 3GPP, METIS, and mmMAGIC [2].

(i) 5GCM UMi street canyon ($6 \leq f \leq 100$ GHz)

LOS;

$$PL = 32.4 + 20 \log(f) + 21 \log(d_{3D}) \quad (18)$$

NLOS;

$$PL = 32.4 + 20 \log(f) + 31.7 \log(d_{3D}) \quad (19)$$

(ii) (ABG)

$$PL = 35.3 \log(d_{3D}) + 22.4 + 21.3 \log(f) \quad (20)$$

(iii) 3GPP UMi street canyon ($0.5 \leq f \leq 100$ GHz)

LOS;

$$PL_1 = 32.4 + 20 \log(f) + 21 \log(d_{3D}),$$

$$PL_2 = 32.4 + 40 \log(d_{3D}) + 20 \log(f) - 9.5 \log(d_{bp}^2 - (h_b - h_m)^2). \quad (21)$$

where $d_{bp} = (4h_b h_m / \lambda)$

Note that PL2 is not exist because dbp over 3,920 m for 28 GHz and 73 GHz.

NLOS;

$$PL = 35.3 \log(d_{3D}) + 22.4 + 21.3 \log(f) - 0.3(h_m - 1.5). \quad (22)$$

Option,

$$PL = 32.4 + 20 \log(f) + 31.9 \log(d_{3D}). \quad (23)$$

(iv) METIS

LOS;

$$L_1 = 31.34 + 20 \log(f) - 1.38 \log(f) + 22 \log(d_{3D}),$$

$$10_m \leq d_{3D} \leq d_{bp} \quad (24)$$

where

$$d_{bp} = 0.87 \exp(-\log(f))4(h_{BS} - 1m)(h_{UE} - 1m)/(0.65\lambda). \quad (25)$$

Note that PL_2 is not exist (d_{bp} over 289 m for 28 GHz and 73 GHz).

NLOS; ($0.45 \leq f \leq 6$ GHz) not exist

(v) mmMAGIC

LOS;

$$PL = 32.9 + 20.8 \log(f) + 19.2 \log(d_{3D}) \quad (26)$$

NLOS;

$$PL = 31.0 + 20 \log(f) + 45 \log(d_{3D}). \quad (27)$$

The results show that the LOS of the proposed model and other models provide a little good agreement for single and dual frequency in the range of 3.17–3.23 as shown in Figures 5–7 and Table 5. The proposed models of a single frequency (28 GHz and 73 GHz) provide a minimum of both MAE and σ . All LOS models are close-in free space (CI) except METIS and mmMAGIC. Their path loss exponents before the breakpoint distance, d_{bp} are more than two except in the mmMAGIC model. Note that all models used distances before d_{bp} which are in the range of 289 m–3920 m at the frequencies of 28 GHz and 73 GHz. In the case of NLOS, the results show that the proposed models provide good prediction especially in the case of hard routes compared with other models as shown in Figures 5–7 and in Table 6, while the ABG models (floating intercept) also provide the

TABLE 6: Comparison of NLOS path loss models.

Name	NLOS models	MAE of Route (STDEV)		
		Hard	Soft	All
5GCM UMi street canyon	(i) Option (ABG)	10.46 (5.70)	4.70 (3.94)4	7.65 (5.42)
		6.56 (5.77)	.71 (3.76)	7.89 (5.45)
3GPP UMi street canyon	(i) Option (CI)	11.23 (5.81)	4.75 (3.65)	9.72 (6.45)
		10.08 (5.68)	4.84 (4.10)	7.49 (5.33)
METIS	None ($0.45 \leq f \leq 6$ GHz)	—	—	—
mMAGIC	(i) Soft	15.25 (5.93)	28.79 (6.10)	21.19 (8.73)
	(ii) Hard	5.04 (4.0)	3.52 (3.15)	—
	(iii) All	—	—	7.51 (5.47)
Proposed (28 GHz)	(i) Soft	—	3.76 (3.59)	—
	(ii) Hard	4.2 (3.75)	—	6.47 (4.75)
	(iii) All	—	—	—
Proposed (73 GHz)	Option (ABG)	—	4.34 (3.53)	—
	(ii) Hard	4.46 (3.79)	4.38 (3.47)	—
	Option (ABG)	4.45 (3.81)	—	6.72 (4.91)
Proposed (dual freq.)	(iii) All	—	—	6.78 (4.88)
	Option (ABG)	—	—	—

best MAE of 4.45, 4.38, and 6.78 of hard, soft, and all-NLOS routes, respectively.

The arbitrary constants β of the proposed ABG models are lower than free space (32.4) while its arbitrary constants α (PLE) are higher than the free space (2.0) because these values are the characteristics of the NLOS environments. Note that the 5GCM and 3GPP models provide good agreement (MAE of 4.7 dB and 4.75 dB) only for soft routes. However, in the case of the hard route, they provide large errors with an MAE of 10.46 dB and 11.23 dB for 5GCM and 3GPP, respectively. The mmMAGIC model provides an over prediction, especially for soft routes, with 28.79 dB, as shown in Table 6.

The correction term of the receiving antenna height in the 3GPP NLOS model (equation (22)) does not provide the large MAE for the hard route because the height of the receiving antennas (2.0 m and 4.06 m above ground) are below the height of the buildings. The dominant waves are attenuated from multidiffraction at the corner of the buildings. The path loss exponents, or $\alpha/10$ of NLOS, are in the range of 3.17–3.53 for general models, while the proposed models are in the range of 3.66–3.71 for the hard routes. This makes them provide good agreement for the hard route.

Note that the mmMAGIC model provides the largest path loss exponent of 4.5 so it makes an over estimated prediction for both soft and hard routes. The other models provide the best prediction only the soft routes except for the mmMAGIC model. The proposed models for dual frequency (CI and ABG) provide no significant difference of MAE between soft routes and hard routes.

5. Conclusions

The researchers present an accurate empirically based path loss model with route classification for high band frequency of 5G wireless communication network. Propagation path routes are mainly classified into the line of sight (LOS) and non-line-of-sight (NLOS). The NLOS consists of 2 routes, namely, Hard_NLOS and Soft_NLOS. Their path loss models are investigated. The path loss models include free-space loss and multiscreen diffraction loss together with the reflection of the building blocks. However, these NLOS models can be combined into a single formula. The path loss models were fitted with measured path loss data at frequencies of 28 GHz and 73 GHz. The researchers compared the proposed model with four 5G empirical models of both CI (CIF) and ABG types, namely, 5GCM, 3GPP, METIS, and mmMAGIC. The results show that the proposed NLOS models provide a good prediction, especially for the hard routes compared with the conventional models, while LOS models provide the same prediction as the other models.

Data Availability

The data used to support the findings of this study are available from the corresponding author upon reasonable request.

Disclosure

The funder was involved in the manuscript writing, editing, approval, or decision to publish.

Conflicts of Interest

The authors declare that they have no conflicts of interest.

Acknowledgments

The research was performed as part of the employment of the authors, Mahidol University.

References

- [1] T. S. Rappaport, F. Gutierrez Jr, E. Ben-Dor, J. N. Murdock, Y. Qiao, and J. I. Tamir, "Broadband millimeter-wave propagation measurements and models using adaptive-beam antennas for outdoor urban cellular communications," *IEEE Transactions on Antennas and Propagation*, vol. 61, no. 4, pp. 1850–1859, 2013.
- [2] T. S. Rappaport, Y. Xing, G. R. MacCartney Jr, A. F. Molisch, E. Mellios, and J. Zhang, "Overview of millimeter wave communications for fifth-generation (5G) wireless networks—with a focus on propagation models," *IEEE Transactions on Antennas and Propagation*, vol. 65, no. 12, pp. 6213–6230, 2017.
- [3] T. S. Rappaport, G. R. MacCartney, M. K. Samimi, and S. Sun, "Wideband millimeter-wave propagation measurements and channel models for future wireless communication system design," *IEEE Transactions on Communications*, vol. 63, no. 9, pp. 3029–3056, Sept. 2015.
- [4] M. K. Samimi, T. S. Rappaport, and G. R. MacCartney Jr, "Probabilistic omnidirectional path loss models for millimeter-wave outdoor communications," *IEEE Wireless Communications Letters*, vol. 4, no. 4, pp. 357–360, 2015.
- [5] S. Sun, T. S. Rappaport, T. A. Thomas et al., "Investigation of prediction accuracy, sensitivity, and parameter stability of large-scale propagation path loss models for 5G wireless communications," *IEEE Transactions on Vehicular Technology*, vol. 65, no. 5, pp. 2843–2860, 2016.
- [6] K. Haneda, N. Omaki, T. Imai, L. Raschkowski, M. Peter, and A. Roivainen, "Frequency-agile pathloss models for urban street canyons," *IEEE Transactions on Antennas and Propagation*, vol. 64, no. 5, pp. 1941–1951, 2016.
- [7] A. I. Sulyman, A. Alwarafy, G. R. MacCartney Jr, T. S. Rappaport, and A. Alsanie, "Directional radio propagation path loss models for millimeter-wave wireless networks in the 28-60-and 73-GHz bands," *IEEE Transactions on Wireless Communications*, vol. 15, no. 10, pp. 6939–6947, 2016.
- [8] A. Karttunen, C. Gustafson, A. F. Molisch et al., "Path loss models with distance- dependent weighted fitting and estimation of censored path loss data," *IET Microwaves, Antennas & Propagation*, vol. 10, no. 14, pp. 1467–1474, 2016.
- [9] S. Hur, F. Member, S. Baek et al., K. H, J. Park, Member proposal on millimeter-wave channel modeling for 5G cellular system," *IEEE J. Selected topics in Sig. Proc.*, vol. 10, no. 3, pp. 454–469, 2016.
- [10] X. Zhang and J. G. Andrews, "Downlink cellular network analysis with multi-slope path loss models," *IEEE Transactions on Communications*, vol. 63, no. 5, pp. 1881–1894, 2015.

- [11] O. J. Pandey and R. M. Hegde, "Node localization over small world WSNs using constrained average path length reduction," *Ad Hoc Networks*, vol. 67, pp. 87–102, 2017.
- [12] H. H. Xia, "A simplified analytical model for predicting path loss in urban and suburban environments," *IEEE Transactions on Vehicular Technology*, vol. 46, no. 4, pp. 1040–1046, 1997.
- [13] D. Har, H. H. Xia, and H. L. Bertoni, "Path-loss prediction model for microcells," *IEEE Transactions on Vehicular Technology*, vol. 48, no. 5, pp. 1453–1462, 1999.
- [14] D. Har, A. M. Watson, and A. G. Chadney, "Comment on diffraction loss of rooftop-to-street in COST 231- walfisch-ikegami model," *IEEE Transactions on Vehicular Technology*, vol. 48, no. 5, pp. 1451–1452, 1999.
- [15] *COST 231 Urban Transmission Loss Models for Mobile Radio in the 900- and 1800-MHz Band*, 1991.
- [16] J. Walfisch and H. L. Bertoni, "A theoretical model of UHF propagation in urban environments," *IEEE Transactions on Antennas and Propagation*, vol. 36, no. 12, pp. 1788–1796, 1988.
- [17] F. Ikegami, S. Yoshida, T. Takeuchi, and M. Umehira, "Propagation factors controlling mean field strength on urban streets," *IEEE Transactions on Antennas and Propagation*, vol. 32, no. 8, pp. 822–829, 1984.
- [18] K. Guan, Z. Zhong, B. Ai, and T. Kurner, "Semi-deterministic path-loss modeling for viaduct and cutting scenarios of high-speed railway," *IEEE Antennas and Wireless Propagation Letters*, vol. 12, pp. 789–792, 2013.
- [19] A. Bhuvaneshwari, R. Hemalatha, and T. Satyasavithri, "Semi deterministic hybrid model for path loss prediction improvement," *Procedia Computer Science*, vol. 92, pp. 336–344, 2016.
- [20] W. Wang, T. Jost, and R. Raulefs, "A semi- deterministic path loss model for in-harbor LoS and NLoS environment," *IEEE Transactions on Antennas and Propagation*, vol. 65, no. 12, pp. 7399–7404, 2017.
- [21] A. Karttunen, A. F. Molisch, S. Hur, J. Park, and C. J. Zhang, "Spatially consistent street-by-street path loss model for 28-GHz channels in micro cell urban environments," *IEEE Transactions on Wireless Communications*, vol. 16, no. 11, pp. 7538–7550, 2017.
- [22] O. J. Pandey, T. Yuvaraj, J. K. Paul, H. H. Nguyen, K. Gundepudi, and M. K. Shukla, "Improving energy efficiency and QoS of LPWANs for IoT using Q-learning based data routing," *IEEE Transactions on Cognitive Communications and Networking*, vol. 8, no. 1, pp. 365–379, 2022.
- [23] W. Tang, X. Chen, M. Z. Chen et al., "Path Loss Modeling and Measurements for Reconfigurable Intelligent Surfaces in the Millimeter-Wave Frequency Band," *IEEE Transactions on Communications*, vol. 70, pp. 1–18, 2022.
- [24] Y. Chang, S. Baek, S. Hur, Y. Mok, and Y. Lee, "A novel dual-slope mm-wave channel model based on 3D ray-tracing in urban environments," in *Proceeding of the IEEE 25th Annual International Symposium on Personal, Indoor, and Mobile Radio Communication (PIMRC)*, pp. 222–226, Washington, DC, USA, September 2014.
- [25] J. H. Lee, J. S. Choi, J. Y. Lee, and S. C. Kim, "28 GHz millimeter-wave channel models in urban microcell environment using three-dimensional ray tracing," *IEEE Antennas and Wireless Propagation Letters*, vol. 17, no. 3, pp. 426–429, 2018.
- [26] G. R. MacCartney Jr., T. S. Rappaport, M. K. Samimi, and S. Sun, "Millimeter-wave omnidirectional path loss data for small cell 5G channel modeling," *IEEE Access*, vol. 3, pp. 1573–1580, 2015.